LENGTH DEPENDENCE OF FORWARD AND BACKWARD THZ DFG IN A STRONGLY ABSORPTIVE MATERIAL

Yen-Chieh Huang, Ming-Yuen Chuang, Yen-Hou Lin, Ching-Han Lee, Tsong-Dong Wang, Yen-Yin Lin, and Fan-Yi Lin
Department of Electrical Engineering, National Tsinghua University, Hsinchu 30013, Taiwan

ABSTRACT

Some believes that the useful length of THz different frequency generation (DFG) in a highly absorptive material is comparable to the absorption length of the THz wave. We show in theory and experiment that it is only true for backward THz DFG. For forward DFG with strong idler absorption, the THz wave can continue to grow with the length of a DFG crystal.

Keywords: difference frequency generation, THz wave, lithium niobate

1. INTRODUCTION

One popular approach to generate coherent THz waves is difference frequency generation (DFG) of two input laser fields in a nonlinear optical material. However, owing to the vast difference in wavelengths for the mixing waves, a nonlinear optical material is often transparent to optical waves but absorptive to the THz wave. A typical example is the THz DFG in lithium niobate. It has been widely believed that the useful DFG length is on the order of the THz absorptive length in such a strongly absorptive nonlinear optical material[1,2]. This notion has prompted a number of techniques to couple out the THz waves as fast as possible for THz DFG in lithium niobate[3], in spite of the possibility of collinear phase matching in periodically poled lithium niobate. In this paper, we show in theory and experiment that the useful length of forward THz DFG in a highly absorptive material is not limited to a crystal length comparable to the absorption length. However, with absorption exceeding parametric gain, the THz output power from backward THz DFG indeed saturates in a crystal length comparable to the THz absorption length.

2. THOERY

Assume plane-wave like solutions for DFG in a 2nd-order nonlinear optical material, $\widetilde{E}_i(t,z) = \mathrm{Re}[\overline{E}_i(z)e^{j\omega_i t - jk_i z}]$, where the subscript $i = p$, s, and THz denotes the pump, signal, and THz (idler) waves, respectively, $\overline{E}(z)$ is a slowly varying envelope field, t is the time variable, ω is the angular frequency of the wave, and k_i is the wave number of wave i. With idler absorption at the THz frequencies, the coupled wave equations for THz DFG are given by

$$\frac{\partial \overline{E}_{THz}}{\partial z} = \mp j\kappa_{THz}\overline{E}_p\overline{E}_s^* \mp \frac{\alpha_{Thz}}{2}\overline{E}_{THz} \tag{1}$$

$$\frac{\partial \overline{E}_s}{\partial z} = -j\kappa_s\overline{E}_p\overline{E}_{THz}^* \tag{2}$$

$$\frac{\partial \overline{E}_p}{\partial z} = -j\kappa_p\overline{E}_s\overline{E}_{THz} \tag{3}$$

where α_{THz} is the absorption coefficient of the THz wave, E^* is the complex conjugate of E, and $k_i = \omega_i d_{eff}/(c_0 n_i)$ with d_{eff}, c_0, and n being the effective nonlinear coefficient, the velocity of light in vacuum, and refractive index,

Nonlinear Frequency Generation and Conversion: Materials, Devices, and Applications X, edited by Konstantin L. Vodopyanov, Proc. of SPIE Vol. 7917, 79170I · © 2011 SPIE
CCC code: 0277-786X/11/$18 · doi: 10.1117/12.875948

respectively. In Eq. (1), the + and − denote the backward and forward THz waves, respectively. In the following we solve the THz photon flux density normalized to the seeded signal photon flux density, or $\bar{\phi}_{THz} = \phi_{THz} / \phi_s(0)$, subject to the undepleted pump condition $\partial \bar{E}_p / \partial z = 0$.

2.1 Forward THz Difference Frequency Generation

Without pump depletion, Eqs. (1,2) can be solved to give the output photo flux density of the forward THz wave from a DFG material of length *L*, given by[4]

$$\bar{\phi}_{THz} = e^{-\alpha_{THz} L/2} \frac{\Gamma^2}{g_f^2} \sinh^2(g_f L), \tag{4}$$

where $g_f^2 \equiv \Gamma^2 + (\alpha_{THz}/4)^2$ with Γ being the parametric gain coefficient without absorption. In the regime of strong absorption $A \equiv (\alpha_{THz}/4\Gamma)^2 >> 1$ and long crystal length $\alpha_{THz} L/2 >> 1$, Eq. (4) reduces to

$$\bar{\phi}_{THz} \approx \left(\frac{2\Gamma}{\alpha_{THz}} \right)^2 e^{(4\Gamma^2/\alpha_{THz})L}, \tag{5}$$

This regime is most interesting, because Eq. (5) predicts an exponential growth rate despite strong idler absorption. Figure 1 shows Eq. (4) (continuous curve) and Eq. (5) (dashed curve) versus a normalized crystal length $\bar{L} \equiv \alpha_{THz} L$ for A = 10. Physically $\bar{L}$ is a crystal length in units of THz absorption length. In lithium niobate, the absorption coefficient is about 20 cm^{-1} at 1.5 THz[5]. A 5-cm long lithium niobate crystal is about the length of 100 absorption lengths. It is seen from Fig. 1 that that THz output power shows no saturation but monotonically increases with the crystal length. Owing to the paired production of the signal and idler photons, the parametric gain supplied to the freely propagating signal wave has assisted the growth of the idler wave.

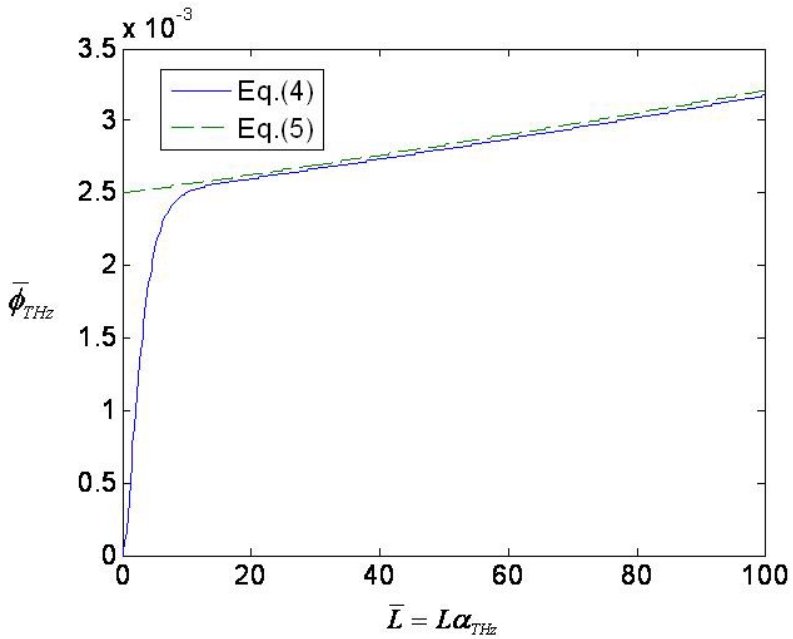

Figure 1. Output photon flux density of the forward THz wave versus crystal length in units of the THz absorption length for the exact solution Eq. (4) and approximate solution Eq. (5). Despite a strong idler absorption of A = 10 assumed in this plot, the THz power shows no saturation but increases with the length of the DFG material.

2.2 Backward THz DFG

Without pump depletion, it can be solved from Eqs. (1, 2) that the output photon flux of the backward THz wave at $z = 0$ from a DFG material of length L is given by

$$\bar{\phi}_{THz} = \frac{\sin^2 g_b L}{\cos^2(g_b L - \varphi)} \tag{6}$$

where $g_b^2 \equiv \Gamma^2 - (\alpha_{THz}/4)^2$ and $\tan\varphi = \alpha_{THz}/(4g_b)$. To have monotonic increase of $\bar{\phi}_{THz}$ over the crystal length L in Eq. (6), one has to ensure the parametric gain exceeding absorption loss $\Gamma > \alpha_{THz}/4$ or $A < 1$, so that g_b is a real number. When the denominator is zero, the backward DFG reaches the threshold of backward wave oscillation. The idler absorption, embedded in g_b and φ, simply increases the pump threshold of the backward parametric oscillation. In the limit of strong THz absorption $A >> 1$, Eq. (3) reduces to

$$\bar{\phi}_{THz} = \left(\frac{2\Gamma}{\alpha_{THz}}\right)^2 (1 - e^{-\alpha_{THz}L/2})^2 \tag{7}$$

Unlike the forward THz DFG, backward THz DFG in the strong absorption limit shows saturation of the output THz power in a crystal length comparable to the THz absorption length. This result is somewhat surprising. It is interesting that, in backward THz DFG, the THz wave propagates back to the beginning of the crystal, where the signal wave is weak and absorption is strong; whereas, in forward THz DFG, the THz wave grows together with the growth of the free propagating signal wave in the forward direction. This explains the very different length dependence for forward and backward THz difference frequency generations with strong idler absorption. Figure 2 plots $\bar{\phi}_{THz}$ from Eq. (6) for the cases of slightly gain exceeding absorption $A = 0.993$ and strong idler absorption $A = 10$. It is seen that for $A = 0.993$ backward wave oscillation is possible as long as the crystal length is long enough. In the strong absorption limit $A = 10$, the output THz wave at $z = 0$ of the crystal saturates in a few absorption lengths.

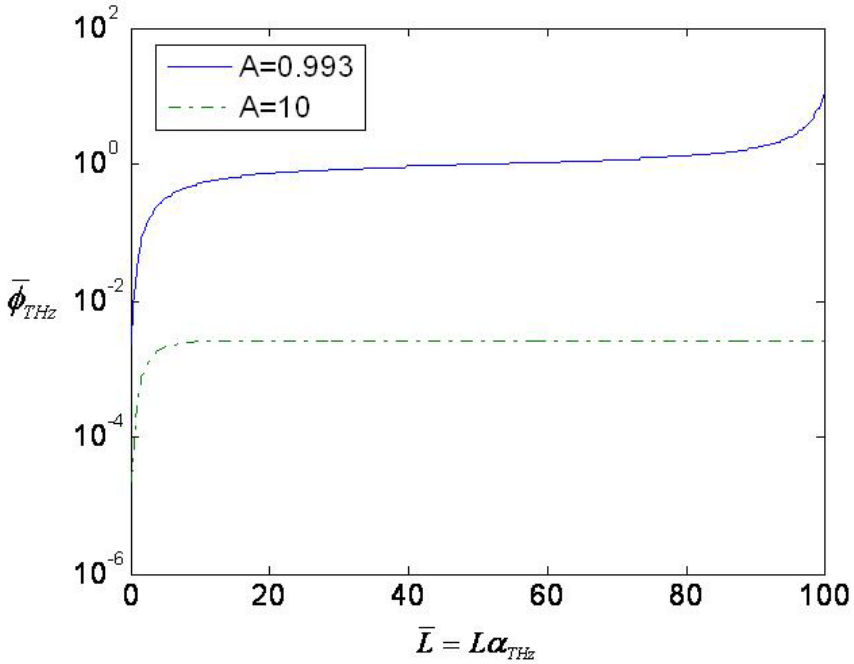

Figure 2. Output photon flux density of the backward THz wave versus crystal length in units of the THz absorption length for slightly gain exceeding absorption $A = 0.993$ and strong absorption $A = 10$. Backward wave oscillation is possible for $A < 1$ as long as the crystal length is long enough. However, for $A > 1$, the THz output power saturates within a crystal length comparable to the THz absorption length.

3. EXPERIMENT

If the THz DFG in a highly absorptive material is limited to a distance comparable to the absorption length of the THz wave, the output power of the THz wave would saturate for a crystal length longer than the absorption length. To investigate the length dependence of the THz output power, we fabricated an array of PPLN crystals with their lengths varying from 1 to 25 mm in 2 mm increment on a 0.5-mm thick, monolithic congruent lithium niobate substrate, as shown in Fig. 3. Each PPLN crystal stripe has a width of 2 mm. The domain period of the PPLN crystals is 65 μm, which is phase matched to the generation of a forward THz wave at 195.7 μm and with pump and signal wavers at 1.551 and 1.539 μm, respectively[6]. At ~200 μm wavelength, the absorption coefficient of lithium niobate is $\alpha_{THz} \sim 20$ cm^{-1}, corresponding to an absorption length of 0.5 mm. For the PPLN crystal, the same grating period is also phase matched to the generation of a backward THz wave at 470 μm for pump and signal waves at about 1.55 μm. In lithium niobate, the absorption length[5] at 470 μm is about 3 mm. The two end faces of the PPLN-array crystal are coated with anti-reflection dielectric layers at the pump and signal wavelengths. The width of the pump and signal pulses is 360 ps, as shown on the left of Fig. 3. We used a previously reported dual-wavelength optical parametric amplifier[6] to generate 9.5-μJ energy in each of the signal and pump components. Both the pump and signal waves were focused to a 130 μm waist radius in the PPLN crystal. With $d_{\text{eff}} \cong 170$ pm/V [7], $n_p = n_s = 2.14$, $n_{\text{THz}} = 5.2$ [6], the parametric gain coefficients are 3.5 and 2.2 cm^{-1} for the forward and backward THz DFG. The index $A \equiv (\alpha_{THz}/4\Gamma)^2$ is calculated to be 2 and 0.14 for the forward and backward DFG, respectively. While keeping the input condition unchanged and measuring the generated THz-wave power in a 4k Si bolometer, we translated the PPLN crystal in the transverse direction and allowed the collinear pump/signal beam to sample the PPLN gratings one at a time. We reversed the pump and signal propagation direction when performing the backward THz DFG experiment.

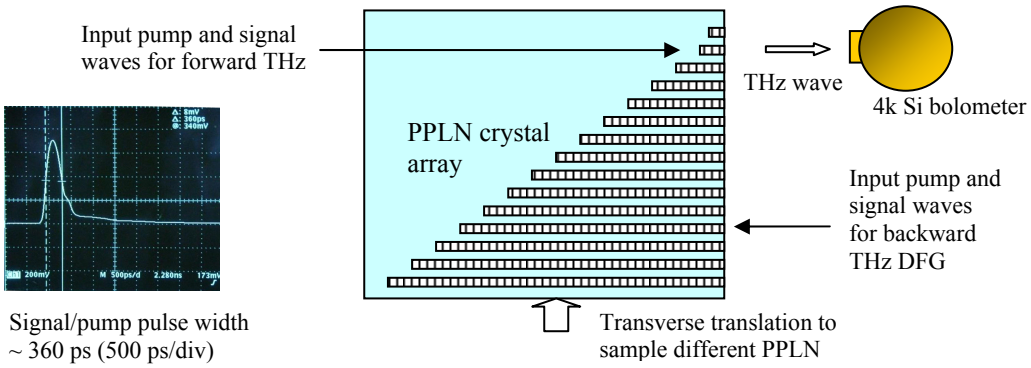

Figure 3. Translation of an array of PPLN crystals of different lengths in the transverse direction allows the study of the length dependence of forward and backward THz DFG in a highly absorptive material. The pump/signal pulse width is 360 ps, as shown on the left of the figure. When performing the backward THz DFG, we reversed the pump/signal direction.

Figure 4 shows the measured forward THz power versus the PPLN crystal length, clearly indicating a monotonic increase of the THz power over a crystal length of about 26 absorption length. The saturation of the curve for $L > 1.3$ cm is due to the walkoff between the optical and THz pulses, because the group velocity mismatch is 103 ps/cm. For the crystal length < 1 mm, the THz signal was buried in the noise of our detector. Although $A = 2$ is not quite in the strong absorption regime for the aforementioned plane-wave model, the fast diffraction of the THz wave should result in a much larger effective A in our experiment. As soon as the THz wave diffracts into a region where there is no pump wave, the THz wave is absorbed immediately in lithium niobate.

Figure 5 shows the measured backward THz power versus the PPLN crystal length, also clearly indicating monotonic increase of the THz power over a crystal length of about 6 absorption lengths. As shown by Fig. 2, this growth of the THz power is not surprising for $A < 1$. For the THz wave not to be absorbed at $z = 0$, the pump pulse has to be long enough to meet with the THz wave at $z = 0$ when the THz wave propagates back from $z = L$ to $z = 0$. This means that the minimum pump pulse width is equal to the one-way time for the pump pulse to propagate from $z = 0$ to L plus the time

for the THz wave to propagate from $z = L$ to $z = 0$. This condition sets a maximum length of 1.5 cm for the PPLN crystal subject to a pump pulse width of 360 ps. Therefore, the walkoff between the THz and the optical pulses once again explains the saturation of the curve for $L > 1.5$ cm in Fig. 5.

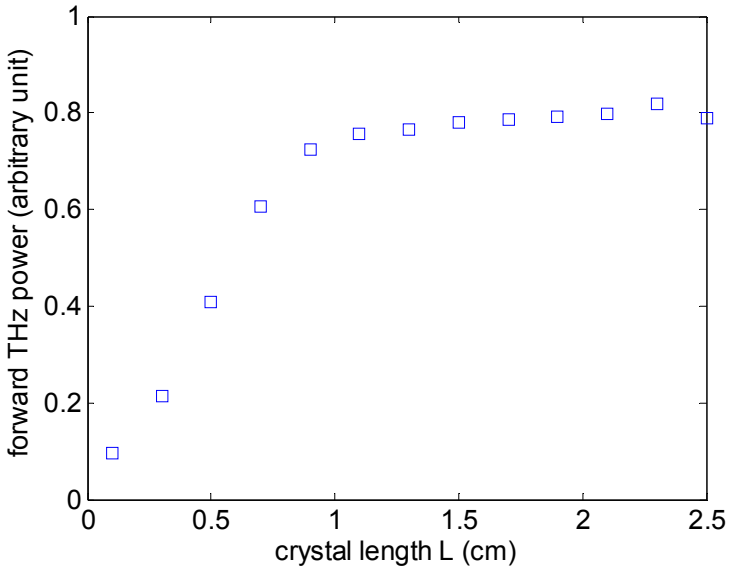

Figure 4 Measured forward THz output power versus PPLN crystal length, indicating monotonic increase of the power over a crystal length of about 26 absorption lengths for A > 2. The group-velocity walkoff between the THz pulse and the optical mixing pulses is 103 ps/cm, which explains the saturation of the curve for $L > 1.3$ cm.

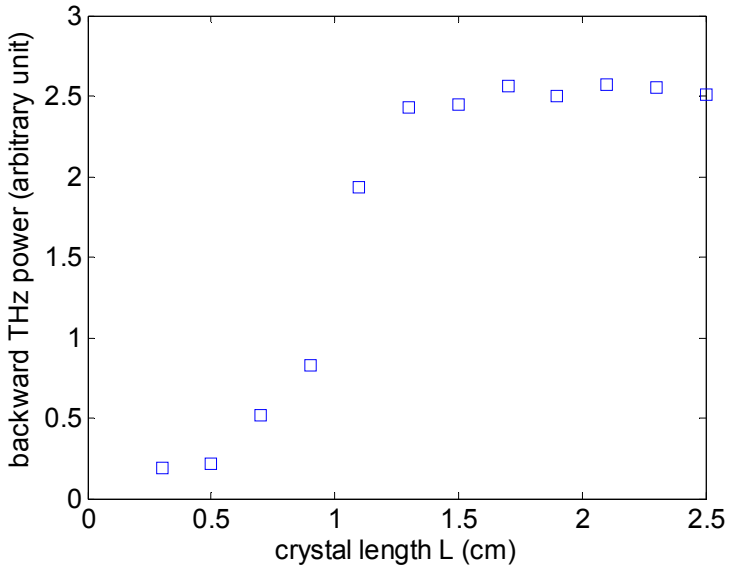

Figure 5 Measured backward THz output power versus PPLN crystal length, indicating monotonic increase of the power over a crystal length of about 5 absorption length for A = 0.14. The walkoff between the THz pulse and the optical mixing pulses explains the saturation of the curves for L > 1.5 cm.

4. CONCLUSION

Our theory and experiment clearly show that forward THz DFG output in a strongly absorptive material is not limited to a crystal length comparable to the THz absorption length, but grows with the crystal length. Since DFG is coherent wave mixing process, the growth of the free propagating signal wave can assist the generation of the highly absorptive THz idler wave in the forward direction. Based on this study, one does not have to couple out the THz wave from lithium niobate as fast as possible when performing THz DFG.

For backward THz DFG, the output power of the backward THz wave indeed saturates over a crystal length comparable to the THz absorption length, if the absorption is stronger than the parametric gain. The backward THz wave propagates back to the beginning of the crystal and experiences an increasingly weak signal wave. As a result, the generation of the THz wave does not benefit from the amplification of the signal wave. However, when the parametric gain exceeds absorption, backward THz DFG can reach the threshold of backward wave oscillation as long as the DFG crystal is long enough.

This work is supported by National Science Council under Contracts NSC 98-2923-M-007 -004 -MY3 and NSC 99-2622-M-007 -001 -CC1.

REFERENCES

[1] J. Hebling, A.G. Stepanov, G. Alm´asi, B. Bartal, J. Kuhl, "Tunable THz pulse generation by optical rectification of ultrashort laser pulses with tilted pulse fronts," Appl. Phys. B **78**, pp. 593–599 (2004).

[2] Y. Avetisyan, Y. Sasaki, H. Ito, "Analysis of THz-wave surface-emitted difference-frequency generation in periodically poled lithium niobate waveguide," Appl. Phys. B **73**, pp. 511–514 (2001).

[3] D. Molter, M. Theuer, and R. Beigang, "Nanosecond terahertz optical parametric oscillator with a novel quasi phase matching scheme in lithium niobate," Optics Express **17**, 6623-6628 (2009).

[4] L. Lefort, K. Puech, G. W. Ross, Y. P. Svirko, and D. C. Hanna, "Optical parametric oscillation out to 6.3 μm in periodically poled lithium niobate under strong idler absorption," Appl. Phy. Lett. **73**, no. 12, pp. 1610–1612 (1998).

[5] L. Pálfalvi, J. Hebling, J. Kuhl, Á. Péter and K. Polgár, "Temperature dependence of the absorption and refraction of Mg-doped congruent and stoichiometric LiNbO3 in the THz range," J. Appl. Phys. **97**, pp. 123505-123511 (2005).

[6] T. D. Wang, S. T. Lin, Y. Y. Lin, A. C. Chiang, and Y. C. Huang, "Forward and backward Terahertz-wave difference-frequency generations from periodically poled lithium niobate," Optics Express **16**, pp. 6471-6478 (2008).

[7] J. Hebling, A.G. Stepanov, G. Almasi, B. Bartal, J. Kuhl, "Tunable THz pulse generation by optical rectification of ultrashort laser pulses with tilted pulse fronts," Appl. Phys. B 78, 593–599 (2004).